Journal of Hydroscience and Hydraulic Engineering
Vol. 28, No.1 May, 2010, 69-85

THE INFLUENCE OF NONUNIFORM SEDIMENT ON DUNE EVOLUTIONS

By

Wandee Thaisiam

Hokkaido University, Sapporo, Japan

Yasuyuki Shimizu

Hokkaido University, Sapporo, Japan

and

Ichiro Kimura

Hokkaido University, Sapporo, Japan

SYNOPSIS

The numerical modeling for non-uniform sediment was performed to simulate the characteristics of sand dunes. By means of the concepts of bed layer model and size fractional transport, the mechanism of grain sorting at various locations on sand dunes can be investigated. It was found that the sand wave formation and its migration process could be reproduced. By using the experimental results, the model provides the satisfactory agreement for grain sorting, wave heights and wave lengths. In addition, the effects of non-uniform sediment on dune evolution were also examined. Under the same hydraulic conditions and mean grain size, the numerical simulations of the non-uniform sediment case were compared with that of the uniform sediment case. The simulated results were consistent with the experimental results which showed that the migration velocities of sand dunes in the non-uniform sediment case are faster than those of the uniform sediment case, and showed that the wave heights of sand dunes of the non-uniform sediment case are smaller than those of the uniform sediment case. The wave lengths of sand dunes of the non-uniform sediment case showed a slight difference with those of the uniform sediment case in the fully developed stage. Moreover, the temporal evolution of sand dune of the non-uniform case was found to be slower than the uniform case.

INTRODUCTION

In the natural rivers, bed material and sediment transport are generally non-uniform. In practice, modeling where non-uniform sediment is considered is rather complicated and time-consuming. As a result, most of the models in the field of river engineering are considered only one grain size of sediment that can represent the non-uniformity of sediment such as a median size. However, many studies have found that considering only one grain size cannot explain some important mechanisms of river morphology sufficiently such as the geometry of

bedforms and their evolutions. One of the essential factors is that one grain size cannot represent realistic bedforms is the effect of grain sorting.

Miwa and Daido (1) performed the experiments on dunes to compare the migration process and sand dune geometry between uniform and non-uniform sediment cases. They also investigated grain sorting at various locations on sand dunes in the experiments of non-uniform sediment. Their experimental results revealed that grain sorting on the upstream part of sand dune crests causes the sediment coarsening on the lee side and, finally, affects the wave height. As a result, with the same mean diameter and hydraulic conditions, the wave height of the non-uniform sediment was found to be smaller than that of the uniform sediment. The wave heights of the non-uniform sediment reached the equilibrium stage in a shorter time than those of the uniform sediment. The wave lengths of dunes with the non-uniform sediment were longer than those of the uniform sediment in the initial formation stage, but the difference in wave lengths decreased when they approached the fully developed stage. The wave lengths of non-uniform sediment were four to six times the mean flow depth. In addition, the migration speed of the non-uniform sediment case was faster than that of the uniform sediment case.

Kleinhans (2) examined the sediment sorting at the lee side of sand dunes. He found that the sorting process can be modeled by considering the following variables: the statistic parameters of sediment mixture (standard deviation, skewness, bimodality) delivered to the brink point, the height of sand dunes or bars relative to the average grain size of the mixture, the flow velocity above the brink point relative to the settling velocity for all grain size fractions, and the frequency of the grain flows. Recently, Blom et al. (3) indicated that the vertical sorting profiles are downward coarsening trend within sand dunes. All of the above mentioned studies show that non-uniform sediment is not only a complicated process which is difficult for modeling, but also significantly affects sand dune morphology.

The numerical models have been applied to the sand dune simulations under the uniform sediment condition. Onda and Hosoda (4) performed the depth averaged flow model considering the effects of vertical acceleration coupled with a non-equilibrium sediment transport model. They succeeded in reproducing the micro-scale sand wave migration process, sand wave geometry characteristics, and flow resistance. Shimizu et al. (5) performed a three-dimensional direct numerical simulation. The model showed a good agreement on flow structures. However, the model is impractical for extending the morphodynamic simulation. Recently, Giri and Shimizu (6) proposed a vertical two-dimensional morphodynamic model with non-hydrostatic and free surface flow for the uniform sediment. In their study, an enhanced k-ε turbulence closure with nonlinear term was incorporated into the hydrodynamic model. Non-equilibrium bed load sediment transport was treated using Eulerian stochastic formulation for the sediment exchange process. They found that the hydrodynamic model with a nonlinear k-ε turbulence closure adequately reproduced flow and vorticity fields in the separation region. The model succeeded in simulating certain features of the dune evolution such as amalgamation and asymmetric geometry. The simulation results were in line with the experimental results.

The morphodynamic numerical model of non-uniform sediment was recently introduced to the field of river engineering. Most of them employed the non-uniform sediment transport in the meso-scale bedform simulations. Bui and Rutschmann (7) performed a 3D numerical model for non-uniform sediment transport in an alluvial channel. In their model, the flow was solved by using the Reynolds averaged Navier-Strokes equations with k-ε turbulence model. The sediment exchange was calculated by using a non-equilibrium sediment transport model. The main features of grain sorting and bed deformation in the channel scale simulation were well reproduced. Wu (8) proposed a depth-averaged two-dimensional numerical modeling for the unsteady flow and the non-uniform sediment transport. The 2D shallow water equations were solved by means of the SIMPLE(C) algorithms with the Rhie and Chow's momentum interpolation technique. The model showed a good agreement with the measured data in meso-scale of bedforms. By using the nonequilibrium sediment transport, all of the above mentioned studies can reproduce the bed

deformation and sediment sorting in the meso-scale of bedform simulations. However, in order to improve our understanding of the inside mechanism of the non-uniform sediment transport and its response to morphology, the micro-scale bedforms should be also investigated. In the case of the micro-scale bedforms such as dunes, the simplified version of flow equations such as the shallow water equations are no longer applicable, and thus more sophisticated equations are necessary.

In the present study, we performed the numerical simulation for sand dunes (micro-scale bedform in the low flow regime) for both the uniform sediment case and the non-uniform sediment case. A vertical two-dimensional flow model with non-hydrostatic and free surface flow proposed by Giri and Shimizu (6) is employed. For the uniform sediment case, we also use the same sediment transport model by Giri and Shimizu (6). For the non-uniform sediment case, the concepts of bed layer model and size fractional transport are applied. Thus, the sediment transport model is divided into two submodels which are the non-uniform sediment transport model and the bed layer model. In this study, we verify our new non-uniform sediment model with the experimental results. Then, the effects of non-uniform sediment will be discussed in the next section by comparing the simulation results of the uniform sediment case and the non-uniform sediment case.

HYDRODYNAMIC MODEL

The governing equations for unsteady two-dimension flow in the Cartesian coordinate system (x,y,t) is transformed to the moving boundary fitted coordinate system (ξ, η, τ) (9). The transformed equations are solved by splitting them into a non-advection and a pure advection term. The non-advection term is solved by using central difference method. The pure advection term is calculated by using a high-order Godunov scheme known as the cubic interpolated pseudoparticle (CIP) technique. The pressure term is resolved by using SOR method. In the turbulence model, a 2^{nd} order non-linear k-ε turbulence closure is employed to reproduce turbulence characteristics in shear flow with separation zone. The time-dependent water surface change computation is used for realistic reproduction of free surface flow over migrating bed forms. The model is able to yield stable and reasonable solutions with a free surface flow condition over the migrating bed forms. The kinematic condition is established along the water surface to compute water surface variation.

The boundary condition at the bed is no slip and a logarithmic expression for near-bed region is adopted. The periodic boundary conditions are employed in the computational domain in both the flow and sediment transport calculations. The output of flow and sediment transport features at the downstream end is set to be input at the upstream end.

SEDIMENT TRANSPORT MODEL

The sediment transport model explicitly takes the turbulence flow into account during the morphodynamic computations. The non-uniform sediment transport model is used for sediment transport calculation, which includes sediment pickup rate, sediment deposition rates, and bed deformation. The bed layer model is applied for grain sorting simulation. The total bed material transport can be modeled by two different approaches, either by dividing the model into bed load and suspended load transport, or by considering only the bed load transport. Presently, our sediment transport computation considers only the bed load transport which is similar to the sediment transport condition of all experiments. In all experiment cases, the suspended load insignificantly dominates in the sediment transport process.

Non-uniform Sediment Transport Model

The sediment transport of non-uniform bed materials normally depends on a potential size fraction transport and is influenced by complicated flow features. The concept of size fraction transport involves dividing bed material into size fractions by considering each size fraction as a uniform material. The sediment transport rate is determined by the summation of the potential transport rate of each size fraction, which is in turn related to its concentration existing in the bed material. The bed material transport rate can be calculated by multiplying the potential transport rate corresponding to a given size fraction with the percentage of material which can be expressed as follows:

$$q_b = \sum_{k=1}^{n} q_{bk} = \sum_{k=1}^{n} P_k \cdot q_k \tag{1}$$

where, q_b = the bed load transport rate per unit width; q_{bk} = the bed load transport of sediment size fraction k per unit width; P_k = the concentration of sediment fraction size k; q_k = the potential transport rate for a given size fraction k; subscripts k and n denote the number and the total number of size fraction respectively.

Tsujimoto and Motohashi (10) advanced a pickup rate formula, which was proposed for uniform sediment by Nakagawa and Tsujimoto (11), for non-uniform sediment by using the critical tractive force for each grain size. The pickup rate for sediment size fraction k is expressed as:

$$p_{sk} = \frac{0.03\tau_{*k}\left(1-0.7\tau_{*ck}/\tau_{*k}\right)^3}{\sqrt{d_k/(\rho_s/\rho-1)g}} \tag{2}$$

where, p_{sk} = the pickup rate of sediment size fraction k; ρ and ρ_s denote fluid and sediment density respectively; τ_{*k} = the dimensionless local bed shear stress of sediment fraction size k; and τ_{*ck} = the dimensionless critical bed shear stress of sediment fraction size k.

The sediment deposition rate is expressed as:

$$p_{dk} = \int p_{sk} f_{sk}(s) ds \tag{3}$$

where, p_{dk} = the deposition rate of sediment fraction size k and $f_{sk}(s)$ = the distribution function of step length. The exponential distribution function of step length of the k^{th} size fraction of bed material by Nakagawa and Tsujimoto (11) applied for non-uniform sediment is expressed as:

$$f_{sk}(s) = \frac{1}{\Lambda_k}\exp\left(-\frac{s}{\Lambda_k}\right) \tag{4}$$

where, Λ_k = the mean step length of sediment size fraction k and s = the distance of sediment motion from the pickup point. On the basis of probability theory, Einstein (12) proposed $\Lambda_k = \alpha d_k$, in which the dimensionless mean step length (α) is an empirical constant. The dimensionless mean step length of non-uniform sediment by Nakagawa et al. (13) was proposed to be 10 to 30. In present study, we used the dimensionless mean step length equal to 30 times of the sediment mean diameter for all Runs. Then, the bed deformation is computed by using the sediment continuity equation which is

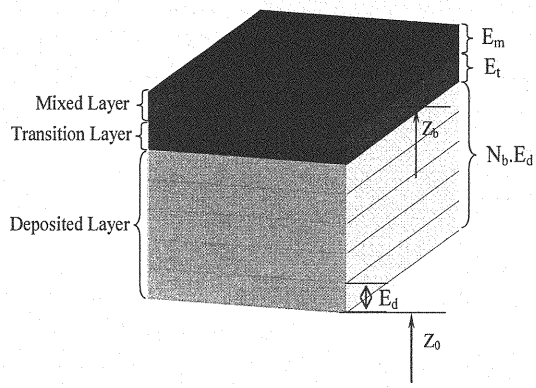

Fig.1 The bed layer model

$$\frac{\partial z_b}{\partial t}+\frac{1}{1-\lambda}\cdot\frac{\partial}{\partial x}\left(\sum_{k=1}^{n} q_{bk}\right)=0 \tag{5}$$

where, z_b = the bed elevation and λ = porosity of bed material.

The Bed Layer Model

The bed layer model proposed by Ashida et al. (14) is employed for the grain sorting simulation of non-uniform sediment in our numerical model. In the bed layer model, bed material is divided into sublayers as shown in Fig. 1.

The mixed layer represents the exchange layer or the top layer containing the bed materials which is active in the transport process. The mixed layer thickness is assumed to be constant and equivalent to the size of d_{90} of initial bed material distribution (14). The transition layer acts as a buffer layer between the mixed layer and the deposited layer. The thickness of the transition layer is a function of time and streamwise direction and is restricted between $0 < E_t \leq E_d$, where, = denotes thickness of transition layer and E_d = thickness of multiple layers. The deposited layer is divided into N_b layers in which the thickness of sublayers is equal to E_d. Therefore, the thickness of the deposited layer is equal to the multiplication of N_b and E_d.

With the initial non-uniform bed material in Fig. 1, the bed elevation is calculated by

$$z_b = E_m + E_t + N_b.E_d + z_0 \tag{6}$$

where, z_b = the bed elevation; E_m = thickness of mixed layer N_b = the total number of sublayers in the deposited layer; and z_0 is the datum elevation.

In present study, we set the initial thickness of bed material equal to 5 centimeters for all Runs. The thickness of the mixed layer (E_m) is set equal to d_{90} of the initial bed material distribution for all Runs. We set the thickness of sublayer in the deposited layer (E_d) equal to 0.25 centimeter. The thickness of the transition layer (E_t) can be then calculated from the initial set up of three parameters and is limited between $0 < E_t \leq E_d$.

In our calculation codes, the non-uniform sediment transport model is used to calculate the sediment pickup rate, the sediment deposition rate and the bed deformation in each calculated cell. In this way, the concentration of sediment size fractions can be calculated from the bed layer model. As the initial bed material condition, we set the grain size distribution of bed material similar to that of the experiments by dividing into five size fractions. A random perturbation field with a small amplitude (0.01 centimeter) is introduced to the initial flat bed. The periodic boundary condition is also employed at the downstream end for a moveable bed calculation. Details of the size

fraction concentration calculation proposed by Ashida et al. (4) can be expressed in four cases as shown in Table 1 in which Δz_b = the bed elevation change between time at t and time at t+Δt; P_{bk} = the concentration of sediment size fraction k in the mixed layer; P_{tk} = the concentration of sediment size fraction k in the transition layer; P_{Nbk} = the concentration of sediment size fraction k in the deposited layer at sublayer *Nbk*; and subscript n and *n+1* denote the calculation time at *t* and *t+Δt* respectively.

EXPERIMENT

Miwa and Daido (1) conducted the experimental studies of the non-uniform sediment. Both the sand wave characteristics and sediment sorting inside sand waves were observed in order to examine the interaction between sediment sorting and the formation of sand waves. The experiment of uniform sediment was also carried out to compare it with the non-uniform sediment case. Experiments were performed in a straight rectangular open channel, 6.5 m long, 0.2 m wide and 0.3 m deep. Four sets of non-uniform sediment were used. The observed data from five cases of the non-uniform sediment experimental study are shown in Table 2. The hydraulic conditions of all experiments are given in the table, in which all parameters were measured after bedforms reached their equilibrium stage. In Table 2, q_w = water discharge per unit width; I_e = the energy slope; u_* = the mean shear velocity; L and Δ denote the wave length and wave height of sand dune respectively.

MODEL VERIFICATION

As described earlier, the numerical model is composed of two main models which are the hydrodynamic model and the non-uniform sediment transport model. The hydrodynamic model was employed and verified in Giri and Shimizu (6). In this study, only the numerical simulation for the non-uniform sediment case is needed to be verified. In the numerical calculation, the computational mesh for flow calculation consists of 302×22 cells. The grid interval in the streamwise direction is equal to 1.0 centimeter, whereas the grid interval in vertical direction is stretched exponentially with the fine grid near bed. The simulation period is 7200 seconds for all Runs which is more than the equilibrium time of all experiments. The time step is 7×10^{-4} seconds. The measured time for sand dune geometries and grain sorting were made after the bed forms reached to the equilibrium stage.

Grain sorting at various locations in sand dunes

Among five experiments, we used the grain sorting observed data at various locations on sand dunes of Run-2 for verifying our sediment transport model. Fig. 2 shows a comparison between the experimental results and our simulated results, and a small figure shows three locations of the measured mixture as Layer I, II and III. Layer I denotes the mixture on the upstream part of dune crests, Layer II denotes the mixture in the trough part of dunes, and Layer III denotes the mixture in the substrate layer. From the experimental results, it was found that Layer I provides the finest mixture among three layers. Layer II which is coarser than Layer I and III because coarse grains was deposited at the lee side, whereas the grain size distribution in Layer III shows no significant changes because it participate weakly in the sediment transport and bed evolution.

Compared with the simulated results, the grain size distribution of bed material inside the sand dunes in layer II and layer III are well reproduced by our new numerical model. This means that our model can illustrate the mechanism of grain sorting. However, we hypothesize that the discrepancy in the result of Layer I may be due to fine sediment that it may have been transported by the mode of suspended load which is excluded in our present model.

Table 1 Cases and conditions for sediment size fraction concentration calculation

case	Bed deformation (Δz_b)	Conditions	Mixed Layer	
			Sediment concentration	thickness
A	aggradation	$E_t^n+\Delta z_b \le E_d$	$P_{bk}^{n+1}=\left(1-\frac{\Delta z_b}{E_m}\right)P_{bk}^n+\frac{\Delta z_{bk}}{E_m}$	d_{90} of initial grain distribution
B	aggradation	$E_t^n+z_b>E_d$	$P_{bk}^{n+1}=\left(1-\frac{\Delta z_b}{E_m}\right)P_{bk}^n+\frac{\Delta z_{bk}}{E_m}$	d_{90} of initial grain distribution
C	degradation	$E_t^n+\Delta z_b>0$	$P_{bk}^{n+1}=P_{bk}^n-\frac{\Delta z_b}{E_m}.P_{tk}^n+\frac{\Delta z_{bk}}{E_m}$	d_{90} of initial grain distribution
D	degradation	$E_t^n+\Delta z_b \le 0$	$P_{bk}^{n+1}=P_{bk}^n+\frac{E_t^n}{E_m}.P_{tk}^n-\frac{E_t^n+\Delta z_b}{E_m}+\frac{\Delta z_{bk}}{E_m}$	d_{90} of initial grain distribution

Table 1 (continuite)

case	Transition Layer		Deposited Layer	
	Sediment concentration	thickness	Sediment concentration	Number of sublayer
A	$P_{tk}^{n+1}=\frac{1}{E_t^{n+1}}\left(E_t^n.P_{tk}^n+\Delta z_b.P_{bk}^n\right)$	$E_t^{n+1}=E_t^n+\Delta z_b$	$P_{Nbk}^{n+1}=P_{Nbk}^n$	$N_b^{n+1}=N_b^n$
B	$P_{tk}^{n+1}=P_{bk}^n$	$E_t^{n+1}=E_t^n+\Delta z_b-E_d$	$P_{Nbk}^{n+1}=P_{tk}^n.\frac{E_t^n}{E_d}+\left(1-\frac{E_t^n}{E_d}\right).P_{bk}^n$	$N_b^{n+1}=N_b^n+1$
C	$P_{tk}^{n+1}=P_{tk}^n$	$E_t^{n+1}=E_t^n+\Delta z_b$	$P_{Nbk}^{n+1}=P_{Nbk}^n$	$N_b^{n+1}=N_b^n$
D	$P_{tk}^{n+1}=P_{Nbk}^n$	$E_t^{n+1}=E_t^n+\Delta z_b+E_d$	$P_{Nbk}^{n+1}=P_{(Nb-1)k}^n$	$N_b^{n+1}=N_b^n-1$

Table 2 Experimental cases and conditions (1)

Run no.	q_w (cm^2/s)	Sediment mean diameter (cm)	d_{90} (cm)	I_e ($x10^{-3}$)	u_* (cm/s)	L (cm)	Δ (cm)
Run-1	350	0.070	0.118	3.50	3.31	30.70	0.67
Run-2	400	0.070	0.118	4.00	3.69	54.00	1.16
Run-3	400	0.076	0.114	2.50	4.50	42.49	1.03
Run-4	350	0.073	0.114	2.50	4.18	42.45	0.88
Run-5	450	0.075	0.114	2.50	5.08	46.50	0.81

From this point, we concluded that the present numerical model shows the capability to reproduce the realistic mechanism of grain sorting inside the sand dunes.

Sand dune geometry

Fig. 3 shows a comparison of the wave heights of sand dunes between the simulated results and the experimental results for Runs 1–5. It was found that the numerical model shows a satisfactory agreement on the wave height predictions with the discrepancy of ±30% in most cases. Fig. 4 shows the comparison of wave lengths of sand dunes between the simulated results and the experimental results for Runs 1-5. The results show that the numerical model provides the under predicted wave lengths of sand dunes in most cases with a discrepancy of ±30%.

EFFECTS OF NON-UNIFORM SEDIMENT

We performed the numerical simulations in both the uniform sediment and the non-uniform sediment cases. We compared the developing process of sand dune, dune geometry and migration velocity in the case of non-uniform sediment with those in the case of uniform sediment. In the uniform sediment case, the model of Giri and Shimizu (6) was employed, while our new model was used for the non-uniform sediment case. We used the experimental conditions and grain size distribution of five Runs as shown in the Table 2 for the non-uniform sediment case, while the mean diameter of sediment and experimental conditions of the same runs were used for the uniform sediment case.

Effect of non-uniform sediment on dune geometry

Fig. 5 and Fig. 6 show a comparison of the wave heights and the wave lengths of sand dunes between the simulated uniform sediment case and the simulated non-uniform sediment case. We use the hydraulic conditions of Runs 1–5 in both the uniform cases and the non-uniform sediment cases. The mean diameter of Runs 1–5 in Table 2 are used in the simulation of the uniform sediment case. The solid line in the figures means that the simulated uniform sediment case and the simulated non-uniform sediment case provide an identical value. If the point is beyond the line, it means that the simulated non-uniform sediment case give a value higher than that of the uniform sediment case.

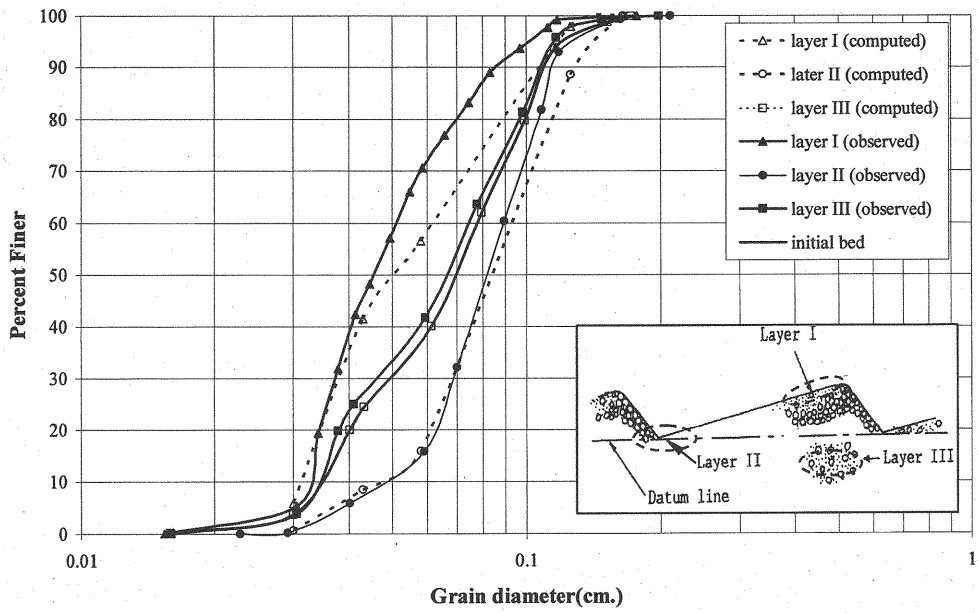

Fig. 2 The comparison of grain size distributions of Run-2
(the locations of measured mixture are as shown in small figure)

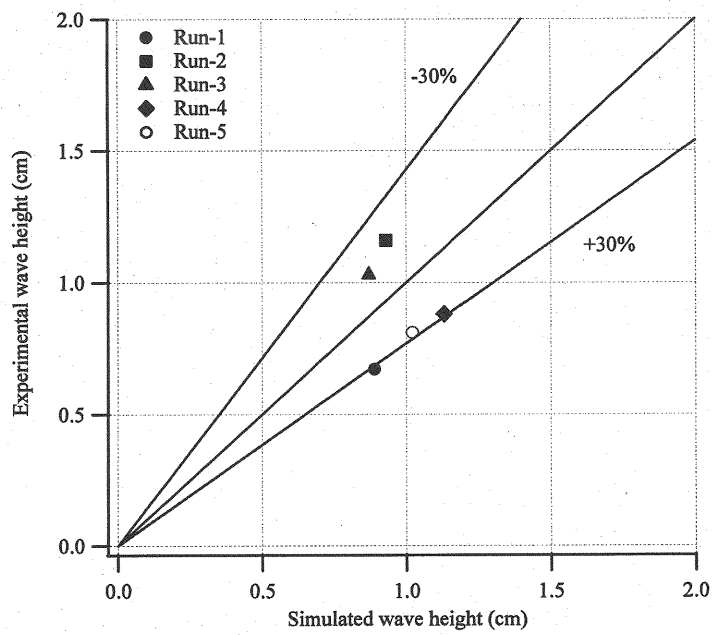

Fig. 3 The comparison of the wave heights of sand dunes between
the simulated results and the experimental results

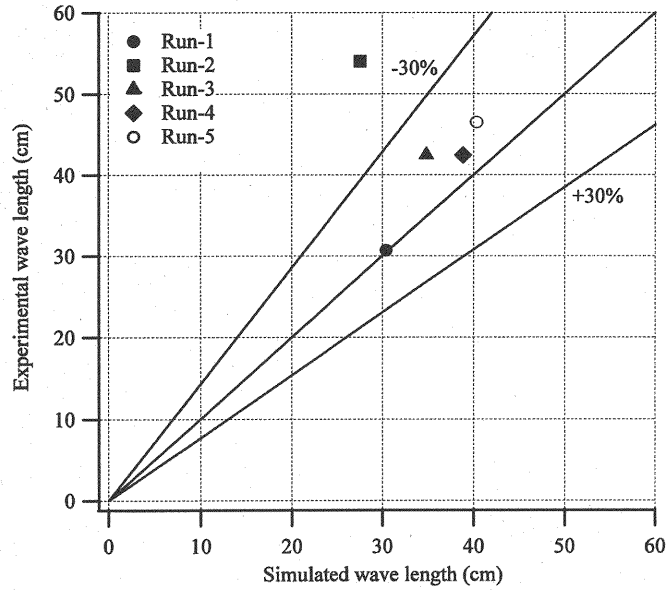

Fig. 4 The comparison of the wave lengths of sand dunes between the simulated results and the experimental results

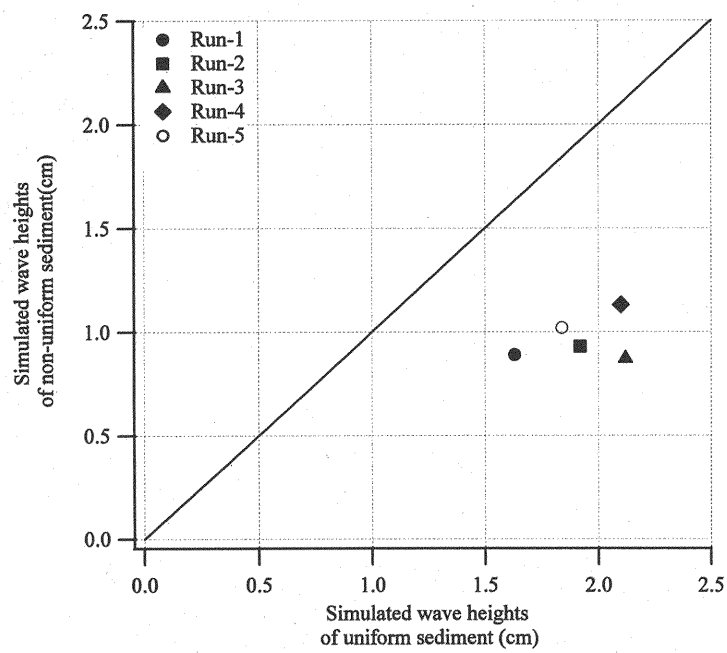

Fig. 5 The comparison of wave heights of sand dunes between the simulated uniform sediment case and the simulated non-uniform sediment case.

Fig. 5 shows that the wave heights of the simulated non-uniform sediment case decrease from those of the uniform sediment case in all Runs (approximately 40%). Miwa and Daido (1) found that the wave heights of non-uniform sediment were approximately 50% less than those of the uniform sediment. Fig. 6 shows that the wave lengths of non-uniform sediment in the fully developed stage show a small difference compared with those of the uniform sediment case in most cases. Again, Miwa and Daido (1) found the same trend as our model results. A comparison results on dune geometry reveals that the non-uniform sediment affects the wave heights of sand dunes, whereas the non-uniform sediment shows a slight effect on the wave lengths of sand dunes in the fully developed stage.

Effect of non-uniform on migration velocity of sand dunes

A comparison of migration velocity of sand dunes between the non-uniform sediment cases and the uniform sediment cases is shown in Fig. 7. The results show that the simulated migration velocities of sand dunes in the non-uniform sediment case are faster than those of the uniform sediment case in most cases. According to Miwa and Daido (1), with the same hydraulic conditions and mean diameter, the migration velocity of the non-uniform sediment case in the experiment is faster than that of the uniform sediment case. Thus, our model shows a satisfactory consistency with the experiment.

Effect of non-uniform sediment on dune evolution

Fig. 8 shows the comparison of the developing process of sand dune in the case of non-uniform sediment with those in the case of uniform sediment. We use the experimental conditions and grain size distribution of Run-3 as shown in Fig. 9 for the non-uniform sediment case, whereas the mean diameter of sediment (d_{50}= 0.076 cm) and experimental conditions of the same run are used for the uniform sediment case. Fig. 8a shows the results of the non-uniform sediment case, and Fig. 8b shows the results of the uniform sediment case. In both cases, we set the domain length equal to 3 meters and use the periodic boundary condition at the downstream end. A random perturbation field with small amplitude (0.01 centimeter) is imposed on the flat bed as the initial condition in both the non-uniform and the uniform cases. From the experimental condition of non-uniform sediment it was found that the sediment was transported only as bedload. Thus we consider only the bedload transport in both the non-uniform and uniform sediment cases.

From the simulation results of the non-uniform sediment case as shown in Fig. 8a, bedforms appear after 2500 s and fully developed at 4500 s, while the grain sorting process appears when bedform geometry is almost fully developed. The simulated wave height and wave length in the fully developed stage are 0.91 cm and 36.8 cm, respectively.

We compared the simulated result of non-uniform case with the observed data at time 4500 s. The simulated wave lengths of bedforms vary from 30.0-42.9 cm (the mean value = 37.8 cm), while the experimental wave length vary from 34.0-60.0 cm (the mean value = 45.7 cm). Thus, the discrepancy is about 17%. The simulated wave heights vary from 0.8-1.1 cm (the mean value = 0.85 cm), while the experimental wave heights vary from 0.75-1.2 cm (the mean value = 1.0 cm). The discrepancy is about 18%. Thus, the present model shows a good consistency with the experiment on the temporal evolution of dunes. In addition, the simulated results show that finer grains are located in a small size of dunes, while the coarser grains are located in large dunes. With the use of non-equilibrium sediment transport model, proposed by Tsujimoto and Motohashi (10), the smaller dimensionless mean step length provides the smaller wave height and wave length of sand dune. We set the dimensionless mean step length equal to 30 times of sediment mean diameter for all Runs.

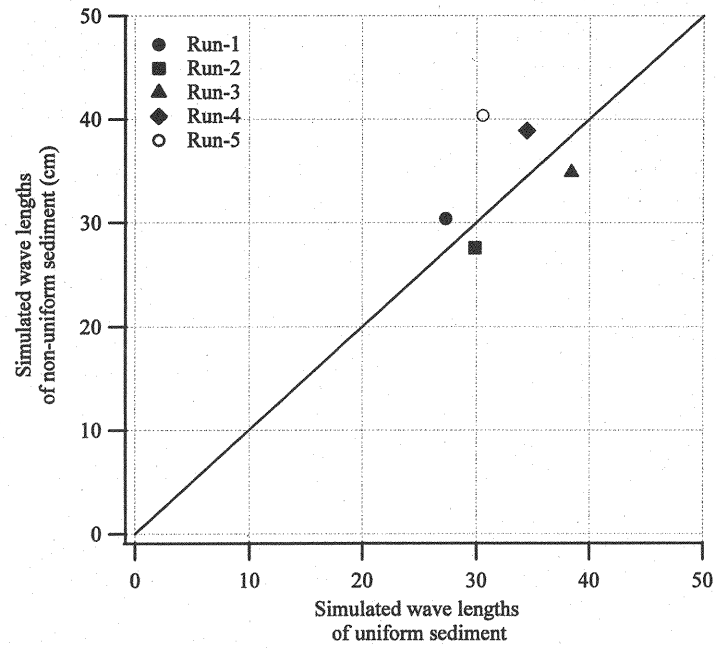

Fig. 6 The comparison of wave lengths of sand dunes between the simulated uniform sediment case and the simulated non-uniform sediment case.

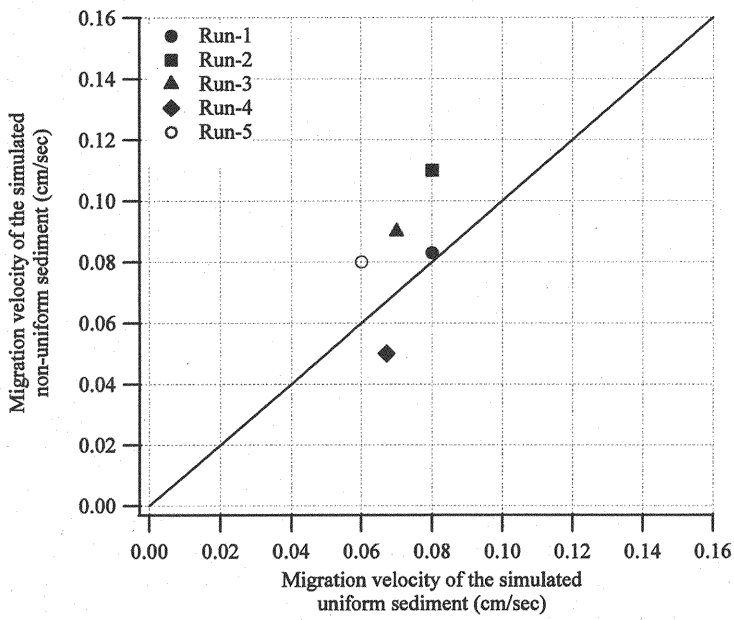

Fig. 7 The comparison of migration velocity of sand dunes between the simulated uniform sediment case and the simulated non-uniform sediment case.

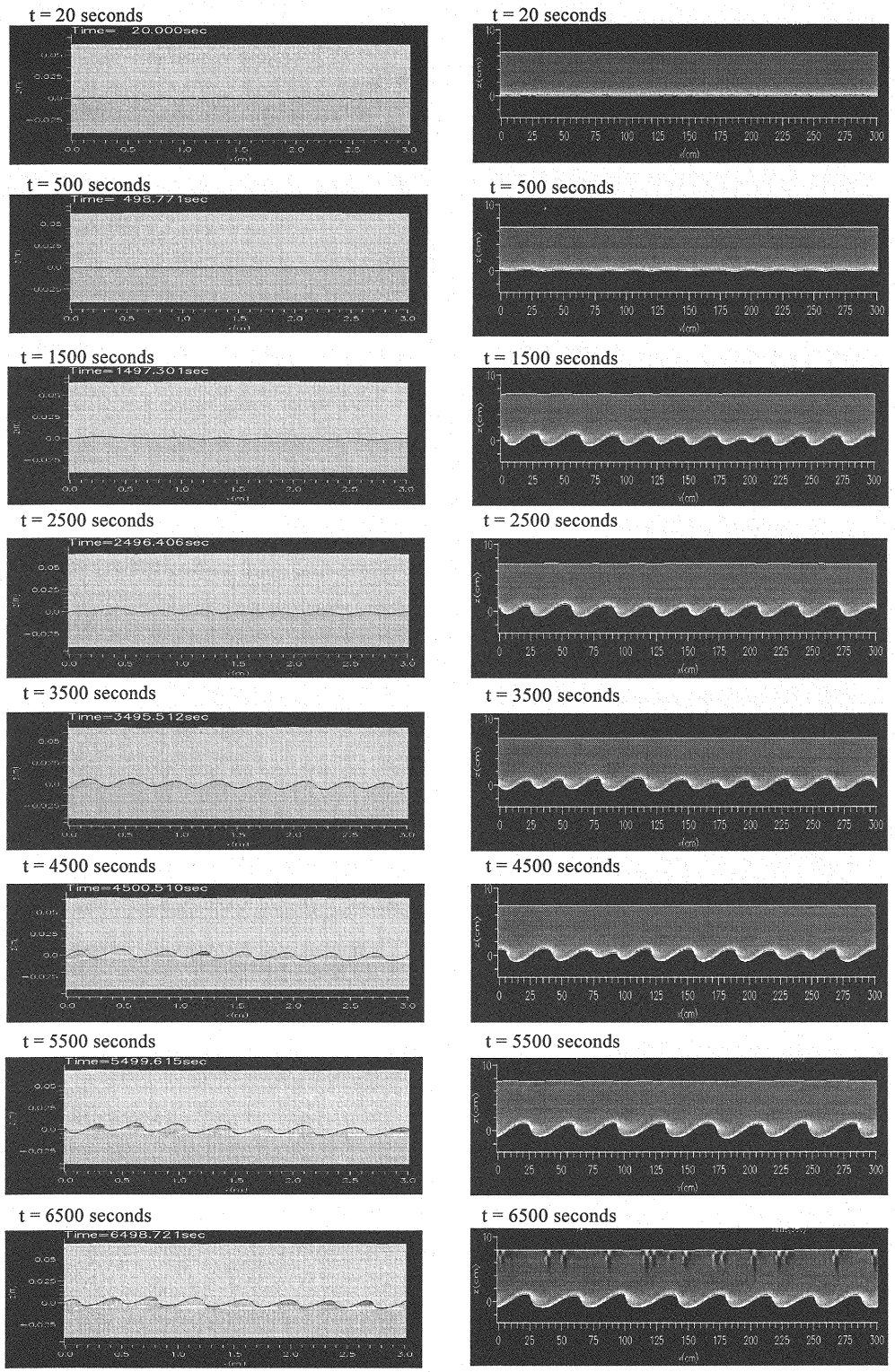

a. Simulated results of nonuniform case

b. Simulated results of uniform case

Fig. 8 The comparison on bedform evolution between the non-uniform sediment case and the uniform sediment case

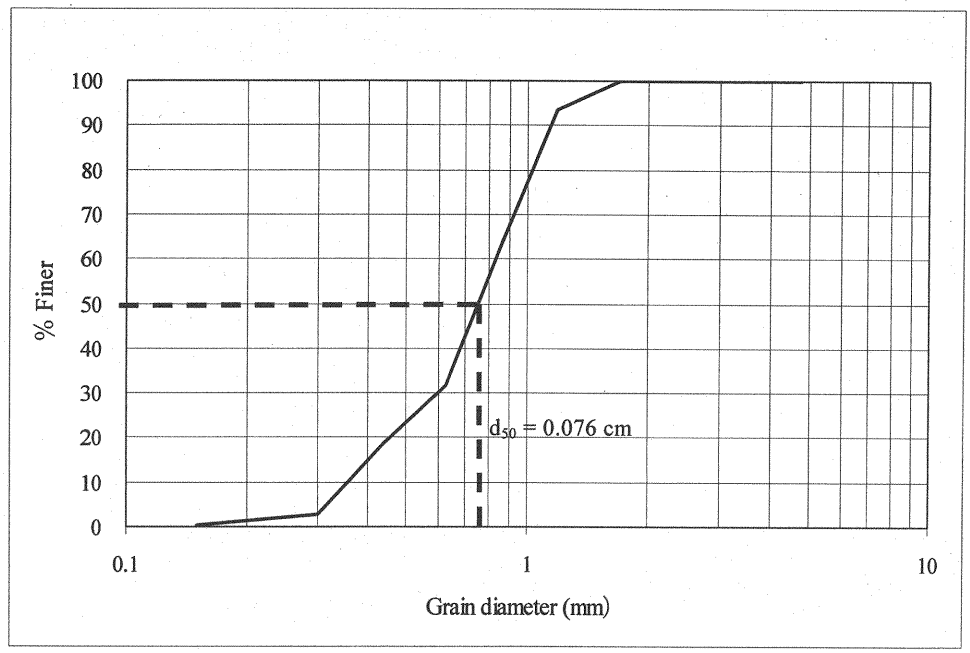

Fig. 9 Grain size distribution of initial bed material of Run-3

Fig. 8b shows the simulated results of the uniform sediment case. Bedforms appear after 1000 s and reach the equilibrium stage after 5500 s. After reaching the equilibrium stage, wave height and wave length of dunes are almost constant. We assume that the constant of bedform geometry in the equilibrium stage is generated by the constant mean step length. The simulated wave height and wave length in the equilibrium stage are 2.12 cm and 38.4 cm, respectively.

The comparison between the non-uniform sediment case and the uniform sediment case shows that the developing process of the non-uniform sediment case is slower than that in the uniform sediment case. Although at the initial stage of the development, the uniform sediment case develops faster than the non-uniform sediment case does. After the wave heights of the non-uniform sediment case are initiated, they abruptly reach the equilibrium stage faster than that of the uniform sediment case. This result is verified by Miwa and Daido (1). In the fully developed stage of bedforms, the simulated wave heights of non-uniform sediment case are approximately 40% less than those of the uniform sediment case. Furthermore, our simulated results agree well with Miwa and Daido (1). The simulated wave lengths of non-uniform case in the fully developed stage are in the range of five to seven times the flow depth, while Miwa and Daido (1) estimated the wave lengths in the range of four to six times the flow depth. The simulated wave lengths of the non-uniform sediment case are longer than those of the uniform case in the initial formation stage, but the wave lengths in both cases show a small variation after reaching the fully developed stage. This result is also in line with the experimental study. In addition, the simulated wave lengths of the non-uniform sediment case remained varied in the small range with each increment of time even after it reaches the fully developed stage, whereas the wave lengths of the uniform sediment case remain settled after the equilibrium stage.

CONCLUSIONS

The numerical model for sand dune simulations under the non-uniform sediment condition was performed and verified with the experimental cases in dune geometry and grain sorting at various locations inside the sand dunes. In addition, a study of the effects of non-uniform sediment on sand dune evolution was conducted. The important conclusions of this study are summarized as follows:

1. The proposed numerical model satisfactorily predicts grain sorting at various locations of sand dunes. Among sediment layers, the upstream part of dune crests in which the sediment is finest showed some discrepancy between the experiment and the model. It is possible that the mode of suspended sediment transport may play a vital role for the discrepancy. The model may need to include the suspended sediment transport in order for better estimating the fine sediment transport.

2. The model shows a good consistency with the wave height of sand dunes between the experiment and the simulation with the discrepancy ±30%, while the wave length of sand dunes was found to be under prediction compared to the experiments with the discrepancy 30% in most cases.

3. The non-uniform sediment transport caused an increase in migration speeds. The initial developing process of non-uniform sediment was found to be slower than that of uniform sediment. However, the wave heights of non-uniform sediment reached the equilibrium stage faster than the uniform sediment case, whereas the wave heights of non-uniform sediment decreased from those of uniform sediment (approximately 40%). The wave lengths of non-uniform sediment were longer than those of the uniform sediment in the initial developing stage but showed a slight difference in the fully developed stage. The wave lengths of the non-uniform sediment remained varied in the small range with the increment of time even after it reaches the fully developed stage, whereas the wave lengths of the uniform sediment are constant after the equilibrium stage.

ACKNOWLEDGEMENTS

We gratefully acknowledge Assco. Prof. Dr. Hiroshi Miwa for providing the unpublished experimental data.

REFERENCES

1. Miwa, H. and Daido, A. : Sand wave development with sediment sorting, Journal of Hydroscience and Hydraulic Engineering, Vol.10 (2), JSCE, pp.39-50, 1992.
2. Kleinhans, M. G. : Sorting in grain flows at the lee side of dunes, Earth-Science Reviews., Vol.65, pp.75–102, 2004.
3. Blom, A., Ribberink, J. S. and H. J. de Vriend : Vertical sorting in bed forms: Flume experiments with a natural and a trimodal sediment mixture, Water Resources Research., 39(2), 1025, doi:10.1029/2001WR001088, 2003.
4. Onda, S. and Hosoda, T. : Numerical simulation on development process of micro scale sand waves and flow resistance Journal of Hydroscience and Hydraulic Engineering., Vol.23 (1), pp.13-26, 2005.
5. Shimizu, Y., Schmeeckle, M. W. and Nelson, J. M. : Direct numerical simulation of turbulence over two-dimensional dunes using CIP methods, Journal of Hydroscience and Hydraulic Engineering, Vol.19(2), pp.85– 92, 2001.
6. Giri, S., and Shimizu, Y. : Numerical computation of sand dune migration with free surface flow, Water Resources Research., 42, W10422, doi:10.1029/2005WR004588, 2006.
7. Bui, Minh Duc and Rutschmann, P. : A 3D numerical of graded sediment transport in nonequilibrium condition, Proc. Conf. on Hydroscience and Engineering (ICHE-2006), Philadelphia, 10-13 Sep., 14p. 2006.

8. Wu, W. : Depth-averaged two-dimensional numerical modeling of unsteady flow and nonuniform sediment transport in open channels, Journal of Hydraulic Engineering, Vol.130(10), pp.1013–1024, 2004.
9. Itakura, T., Yamaguchi, Y., Shimizu, Y., Kishi, T. and Kuroki, M. : Observation of bed topography during the 1981-flood in the Ishikari River, Journal of Hydroscience and Hydraulic Engineering., Vol.4(2), pp.11-19, 1986.
10. Tsujimoto, T. and Motohashi, K. : Static armoring and dynamic pavement, Journal of Hydroscience and Hydraulic Engineering., Vol.8 (1): pp.55-67, 1990.
11. Nakagawa, H., and Tsujimoto, T. : Sand bed instability due to bedload motion, Journal of the Hydraulic Division, Proceedings of the American Society of Civil Engineers, Vol.106(12), pp.2029–2051, 1980.
12. Einstein, H. A. : Formulas for the transport of bed load, Trans. American Society of Civil Engineers., 107, pp.561-597, 1942.
13. Nakagawa, H., Tsujimoto, T. and Nakano, S. : Characteristics of sediment motion for respective grain sizes of sand mixtures, Bull., Disas. Prev. Res. Ints., KyotoUniv. Vol. 32, pp.1-32, 1982.
14. Ashida, K., Egashira, S. and Lui, B. : Numerical calculation of flow and bed evolution in compound channels by a two-layer flow model, the Annuals of the Disaster Prevention Research Institute, Kyoto University, No.35 B-2, pp.41-62, 1992. (in Japanese)

APPENDIX – NOTATION

The following symbols are used in this paper:

d_k = mean diameter of sediment size fraction k

d_{90} = grain diameter at percent finer equal to 90

E_d = thickness of sub-layer in deposited layer

E_m = thickness of mixed layer

E_t = thickness of transition layer

$f_{sk}(s)$ = distribution function of step length of sediment size fraction k

g = gravitational acceleration

I_e = the energy slope

k = number of size fraction

L = wave length of sand dune

n = total number of sediment size fraction

N_b = total number of sub-layer in the deposited layer

P_k = the concentration of sediment size fraction k

p_{dk} = deposition rate of sediment size fraction k

p_{sk} = pickup rate of sediment size fraction k

q_b = bed load transport rate per unit width

q_{bk} = bed load transport of sediment size fraction k per unit width

q_w = the flow discharge per unit width

s = the distance of sediment motion from the pickup point

t = time

u_* = mean shear velocity

z_b = bed elevation

z_0 = the datum elevation

τ_{*k} = dimensionless local bed shear stress of sediment size fraction k

τ_{*ck} = dimensionless critical bed shear stress of sediment size fraction k

ρ_s = sediment density

ρ = fluid density

λ = porosity of bed material

Δ = wave height of sand dunes

Λ_k = dimensionless mean step length of sediment size fraction k

(Received Aug 01, 2009 ; revised Mar 10, 2010)